JACS
JOURNAL OF THE AMERICAN CHEMICAL SOCIETY
Communication
pubs.acs.org/JACS

From Ribbons to Networks: Hierarchical Organization of DNA-Grafted Supramolecular Polymers

Yuliia Vyborna, Mykhailo Vybornyi, and Robert Häner*

Department of Chemistry and Biochemistry, University of Bern, Freiestrasse 3, CH-3012 Bern, Switzerland

Supporting Information

ABSTRACT: DNA-grafted supramolecular polymers (SPs) allow the programmed organization of DNA in a highly regular, one-dimensional array. Oligonucleotides are arranged along the edges of pyrene-based helical polymers. Addition of complementary oligonucleotides triggers the assembly of individual nanoribbons resulting in the development of extended supramolecular networks. Network formation is enabled by cooperative coaxial stacking interactions of terminal GC base pairs. The process is accompanied by structural changes in the pyrene polymer core that can be followed spectroscopically. Network formation is reversible, and disassembly into individual ribbons is realized either via thermal denaturation or by addition of a DNA separator strand.

The creation of functional nanoscale structures represents a major goal of today's nanotechnology. DNA-based materials are of primary interest for the construction of functional platforms.[1−4] Proper choice of the nucleotide sequence provides control over aromatic stacking and hydrogen bonding interactions,[5−7] thus enabling the assembly of systems with a high degree of complexity.[8−11] Approaches toward the preparation of functional DNA materials include the designed DNA self-assembly,[12−15] the grafting of oligonucleotides onto metal nanoparticles (NPs)[16] and other surfaces,[17−19] as well as polymers.[20−23] The latter class, DNA-grafted polymers, has been pioneered by Nguyen and Mirkin and gained increasing attention over the last years.[24,25] We have recently introduced DNA-grafted supramolecular polymers (SPs).[26] These self-assembled structures appear as one-dimensional (1D) ribbons, consisting of an oligopyrenotide core[27] with arrays of single-stranded oligonucleotides appended onto its edges. The noncovalent nature of SPs brings the additional feature of reversibility of the polymerization process.[28−34] Furthermore, it enables the formation of polymers with a high DNA grafting density.[25,26] Herein we describe the hierarchical organization of DNA-grafted SPs. It is shown that individual ribbons assemble into extended networks through a highly cooperative mesh of blunt end DNA stacking interactions.

Chimeric oligomers **Py-a**, **Py-b**, and **Py-c** (Scheme 1) are composed of a heptapyrenotide part and an appended oligonucleotide. They were prepared via solid-phase synthesis, purified by RP-HPLC, and characterized by MS (SI). The two complementary oligonucleotides **1a** (separator strand) and **1b** (connector strand) have the same nucleobase sequence as the corresponding chimeric oligomers **Py-a** and **Py-b**; **1c** is complementary to the oligonucleotide part of **Py-c**.

Scheme 1. Sequences of Chimeric Oligomers, Chemical Structure of Phosphodiester-Linked Pyrenes, and Illustrative Representation of a Folded Chimeric Oligomer

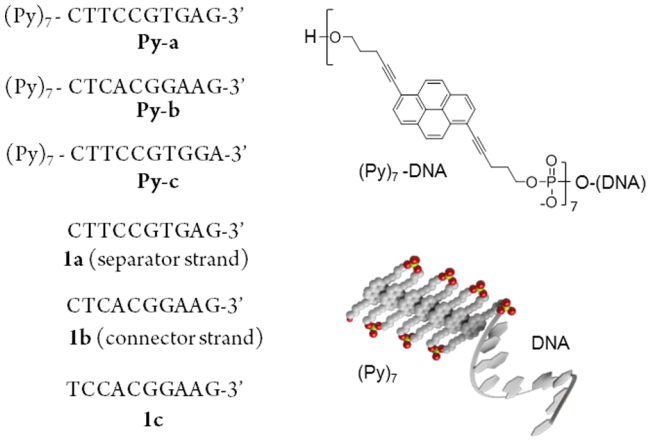

DNA-grafted SPs are typically formed by slow annealing. Thus, a 2 μM solution of **Py-a** in aqueous buffer (10 mM sodium phosphate, pH = 7.0 and 250 mM sodium chloride) is cooled from 95 to 20 °C using a gradient of 0.1 °C/min. Stacking interactions between pyrenes drive the self-assembly of polymeric ribbons. The polymerization process leads to the development of two distinct absorption bands in the UV−vis spectrum at 335 (H-band; $S_0 \rightarrow S_1$ transition) and 305 nm (J-band; $S_0 \rightarrow S_2$ transition; see Figure 1A).[35,36] The assembly/disassembly process is most conveniently followed by changes of the 305 nm band (Figure 1B−D; for monitoring at 260 nm see Figure S11). Figure 1B shows the assembly of ribbons from **Py-a** upon cooling. The polymerization occurs via a single transition that starts at ∼85 °C. The process is reversible, and some hysteresis is observed. Surprisingly, if the same procedure is performed in the presence of the complementary oligonucleotide **1b**, a second transition appears below 30 °C (Figure 1C). The change in the intensity of the J-band reflects a conformational reorganization of the supramolecular pyrene array. The sharpness of this transition, characterized by a full-width at half-maximum (fwhm)[25] value of 1.5 °C (melting) and 2.5 °C (annealing), suggests a high degree of cooperativity. Also this process is reversible and shows hysteresis. In contrast,

Received: September 20, 2015
Published: October 22, 2015

DOI: 10.1021/jacs.5b09889
J. Am. Chem. Soc. 2015, 137, 14051−14054

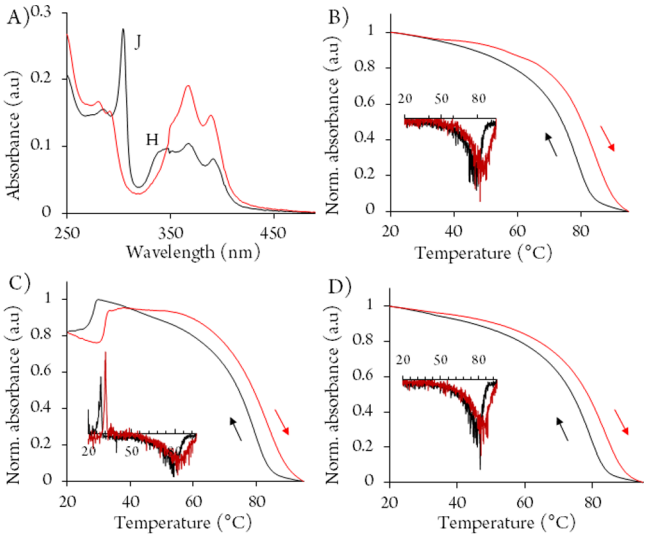

Figure 1. (A) UV−vis of **Py-a** at 20 °C (black) and 95 °C (red). Temperature-dependent change of absorbance at 305 nm of **Py-a** (B), **Py-a*1b** (C), and **Py-a** + **1a** (D). Arrows indicate cooling and heating. Cooling (black) and heating (red) were performed using a 0.1 °C/min ramp. Conditions: 2 μM **Py-a** and 6 μM of **1b** (C) or **1a** (D); 10 mM phosphate buffer, pH = 7.0, 250 mM sodium chloride. The insets in (B−D) show the first derivatives of the corresponding curves.

annealing/melting curves for a system containing **Py-a** and the noncomplementary oligonucleotide **1a** exhibit only a single transition below 85 °C, which coincides with the formation of **Py-a** nanoribbons (Figure 1D).

Circular dichroism (CD) spectroscopy provides further insight in the nature of the transition observed around 30 °C. While the CD spectrum of the **Py-a*1b** system resembles the one of B-DNA below 300 nm, it exhibits a strong exciton-coupled signal (Figure 2A, red curve) in the 300−320 nm

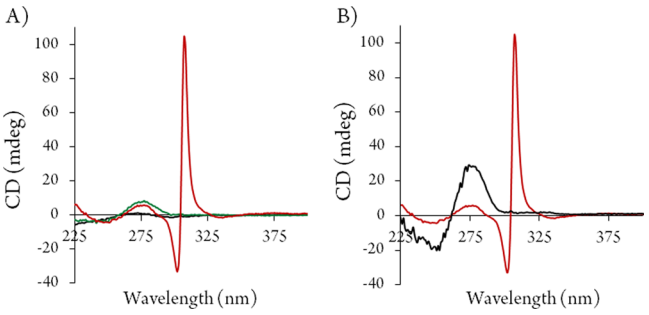

Figure 2. CD spectra at 20 °C. (A) **Py-a** (black), **Py-a** + **1a** (green), **Py-a*1b** (red) prepared by slow annealing (conditions: as in Figure 1). (B) **Py-a*1b** before (red) and after (black) addition of **1a** (conditions: as in Figure 1, except **1a** was used at 12 μM conc.).

region at 20 °C. The bisignate signal (+307/−303 nm) corresponds to the J-band of assembled pyrenes.[37a] Heating to 35 °C leads to the disappearance of the signal (see Figure S2), which clearly shows that it is linked to the transition taking place in this temperature range. The appearance of the exciton coupled signal represents a change in the relative orientation of the transition dipole moments.[37b] This suggests that the stacking arrangement of the pyrenes, and hence, their electronic interaction is altered during the observed process. In contrast, the samples prepared either from **Py-a** alone or **Py-a** + **1a** are CD silent in the 300−320 nm region (Figure 2A, black and green curves). Thus, the low temperature transition only occurs when **1b** (connector strand) is hybridized to the DNA part of **Py-a**.

Atomic force microscopy (AFM) was used to correlate the spectroscopic data with the morphological appearance of aggregates. Supramolecular polymers were deposited and visualized on amino-modified mica surface. The self-assembly of **Py-a** results in the formation of ribbons that exhibit a length of several hundred nanometers and are randomly distributed on the surface (Figure 3A). The **Py-a** + **1a** mixture leads to

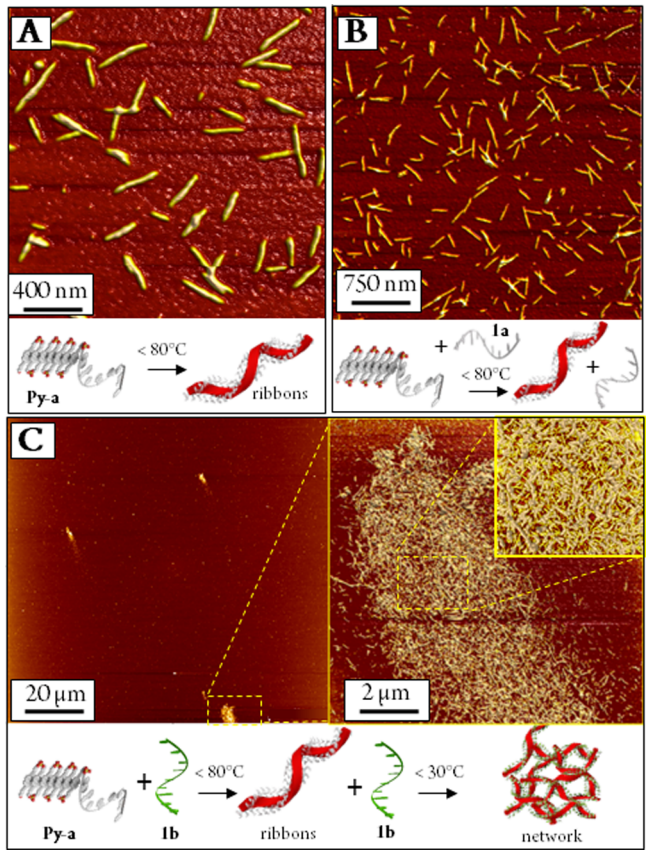

Figure 3. AFM images and illustration of supramolecular assemblies formed from **Py-a** (A), **Py-a** + **1a** (B), and **Py-a*1b** (C). Conditions as in Figure 2.

identical results (Figure 3B). In the complementary **Py-a*1b** system, however, polymers exist as high-density networks (Figure 3C), reminiscent of haystacks in a field, rather than as individual ribbons. The formation of networks is confirmed by transmission electron microscopy (TEM; Figure S10).

The two transitions appearing in the annealing curves of **Py-a** in the presence of complementary oligonucleotide **1b** reflect the hierarchical structural organization of chimeric oligomers. Based on the combined spectroscopic and morphologic data, we propose a model for network formation as illustrated in Scheme 2. The first transition is due to the formation of nanoribbons via supramolecular polymerization of **Py-a**. The second cooperative transition occurs only in the presence of the complementary oligonucleotide **1b**. Hybridization of **1b** to the single-stranded oligonucleotides grafted onto the pyrene nanoribbons results in the formation of duplexes that are arranged along the edges of the ribbons (see Scheme 2) and contain GC base pairs at their termini. Cooperative interactions

DOI: 10.1021/jacs.5b09889
J. Am. Chem. Soc. 2015, 137, 14051−14054

Scheme 2. Illustration of Hierarchical Self-Assembly Process[a]

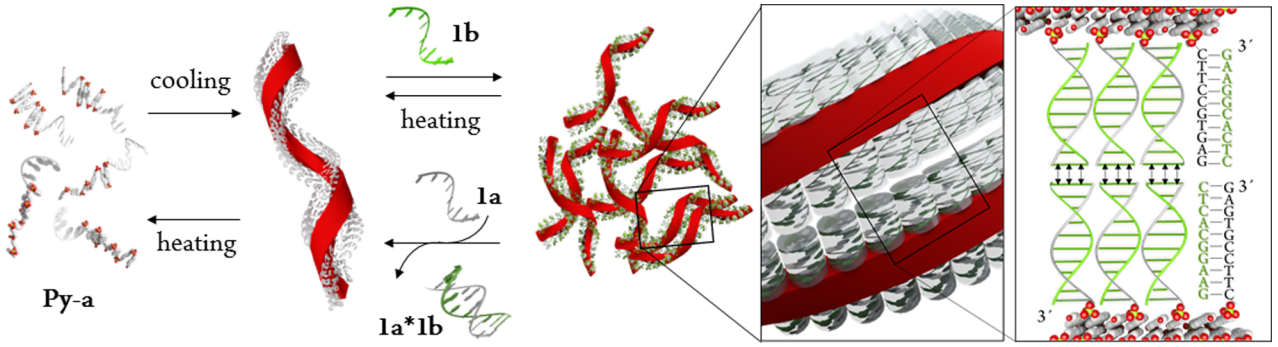

[a]Nanoribbons are formed through assembly of chimeric oligomers (**Py-a**) in a first step. Subsequent hybridization of oligonucleotide **1b** to the DNA part of the nanoribbons leads to formation of duplexes containing GC base pairs at their ends. Networks are then formed via cooperative blunt end stacking interactions.

between individual ribbons through coaxial stacking of the blunt-ended GC base pairs lead to network formation. We assume that each ribbon, through short patches of a few GC basepairs, is connected to neighboring ribbons; long-range collinear stacking of ribbons is unlikely. The importance of blunt end stacking interactions for the controlled assembly of DNA nanostructures and devices is well documented.[5,6,15,38−40] Coaxial stacking[41−44] of GC base pairs is significantly stronger than of AT base pairs.[45,46] This is also observed in the present case. In oligomer **1c**, the two 3′-terminal bases are switched in comparison to **1b** (Scheme 1). The annealing curve of oligomer **Py-c** in the presence of **1c** shows only a single transition occurring at 80 ± 5 °C (Figure S7). Thus, the blunt-ended AT base pairs, which are formed by hybridization of **1c** with **Py-c**, do not support network formation due to decreased stability of their coaxial stacking interactions. The influence of base composition on network formation was further elucidated by a series of control oligonucleotides differing in length and base sequence (see Scheme S1). The data show that mismatches, overhanging nucleobases, or shorter duplexes have the expected negative impact on the formation and the stability of networks. Furthermore, the hierarchical assembly is not limited to the **Py-a*1b** pair. Identical results are obtained with the combination **Py-b*1a** (Figure S1), which also contains GC blunt ends.

The supramolecular nature of the interaction of nanoribbons allows reversing the network formation under isothermal condition, as shown by competition experiments. Thus, addition of the separator strand (**1a**, 2-fold excess over **1b**) to the **Py-a*1b** network at 20 °C results in the disassembly of the aggregates (illustrated in Scheme 2). Formation of the duplex **1a*1b** (T_m = 47 °C, Figure S5) leads to the removal of the connector strand **1b** from the network. Complete disappearance of the network is accomplished within 2 h (Figure S4C). AFM imaging shows only individual ribbons after addition of **1a** (Figure S8). The disassembly process is also confirmed by the disappearance of the CD signal centered around 305 nm (Figure 2B).

In conclusion, we have demonstrated that chimeric pyrene-DNA oligomers assemble into extended networks via a hierarchical assembly pathway. The first step, self-assembly of oligomers into helical nanoribbons, is driven by aromatic stacking interactions among pyrene units. The supramolecular polymerization is independent from the nucleotide sequence of the DNA part. The second step, aggregation of individual nanoribbons into extended networks, only takes place in the presence of a complementary oligonucleotide. Hybridization leads to the formation of duplexes along the helical nanoribbon core. Coaxial stacking interactions of blunt end GC base pairs trigger the formation of a network in a highly cooperative process. The networks can be disassembled by destroying the coaxial stacking interactions either by heating or addition of a separator strand. Supramolecular polymeric networks of this type may be relevant for the development of DNA-based smart materials, such as stimuli-responsive carriers of biologically active agents.

■ ASSOCIATED CONTENT

Supporting Information

The Supporting Information is available free of charge on the ACS Publications website at DOI: 10.1021/jacs.5b09889.

Additional spectroscopic (UV−vis, CD) and microscopic (AFM and TEM) data(PDF)

■ AUTHOR INFORMATION

Corresponding Author

*robert.haener@dcb.unibe.ch

Notes

The authors declare no competing financial interest.

■ ACKNOWLEDGMENTS

This work was supported by the Swiss National Foundation (Grant 200020_149148).

■ REFERENCES

(1) Jones, M. R.; Seeman, N. C.; Mirkin, C. A. *Science* **2015**, *347*, 1260901.
(2) Lu, C. H.; Willner, B.; Willner, I. *ACS Nano* **2013**, *7*, 8320−8332.
(3) Zhang, F.; Nangreave, J.; Liu, Y.; Yan, H. *J. Am. Chem. Soc.* **2014**, *136*, 11198−11211.
(4) Yin, P.; Choi, H. M.; Calvert, C. R.; Pierce, N. A. *Nature* **2008**, *451*, 318−322.
(5) Woo, S.; Rothemund, P. W. *Nat. Chem.* **2011**, *3*, 620−627.
(6) Gerling, T.; Wagenbauer, K. F.; Neuner, A. M.; Dietz, H. *Science* **2015**, *347*, 1446−1452.
(7) Douglas, S. M.; Dietz, H.; Liedl, T.; Hoegberg, B.; Graf, F.; Shih, W. M. *Nature* **2009**, *459*, 414−418.
(8) Bath, J.; Turberfield, A. J. *Nat. Nanotechnol.* **2007**, *2*, 275−284.
(9) Nykypanchuk, D.; Maye, M. M.; van der Lelie, D.; Gang, O. *Nature* **2008**, *451*, 549−552.
(10) Ke, Y.; Ong, L. L.; Sun, W.; Song, J.; Dong, M.; Shih, W. M.; Yin, P. *Nat. Chem.* **2014**, *6*, 994−1002.

DOI: 10.1021/jacs.5b09889
J. Am. Chem. Soc. 2015, 137, 14051−14054

(11) Serpell, C. J.; Edwardson, T. G.; Chidchob, P.; Carneiro, K. M.; Sleiman, H. F. *J. Am. Chem. Soc.* **2014**, *136*, 15767−15774.
(12) Gong, P.; Levicky, R. *Proc. Natl. Acad. Sci. U. S. A.* **2008**, *105*, 5301−5306.
(13) Randeria, P. S.; Jones, M. R.; Kohlstedt, K. L.; Banga, R. J.; de la Cruz, M. O.; Schatz, G. C.; Mirkin, C. A. *J. Am. Chem. Soc.* **2015**, *137*, 3486−3489.
(14) Rafat, A. A.; Pirzer, T.; Scheible, M. B.; Kostina, A.; Simmel, F. C. *Angew. Chem., Int. Ed.* **2014**, *53*, 7665−7668.
(15) Woo, S.; Rothemund, P. W. *Nat. Commun.* **2014**, *5*, 4889.
(16) Cutler, J. I.; Auyeung, E.; Mirkin, C. A. *J. Am. Chem. Soc.* **2012**, *134*, 1376−1391.
(17) Tjong, V.; Tang, L.; Zauscher, S.; Chilkoti, A. *Chem. Soc. Rev.* **2014**, *43*, 1612−1626.
(18) Sassolas, A.; Leca-Bouvier, B. D.; Blum, L. J. *Chem. Rev.* **2008**, *108*, 109−139.
(19) Howorka, S.; Hesse, J. *Soft Matter* **2014**, *10*, 931−941.
(20) Pu, F.; Ren, J.; Qu, X. *Adv. Mater.* **2014**, *26*, 5742−5757.
(21) Kedracki, D.; Safir, I.; Gour, N.; Ngo, K. X.; Vebert-Nardin, C. *Adv. Polym. Sci.* **2012**, *253*, 115−150.
(22) Averick, S. E.; Dey, S. K.; Grahacharya, D.; Matyjaszewski, K.; Das, S. R. *Angew. Chem., Int. Ed.* **2014**, *53*, 2739−2744.
(23) (a) Peterson, A. M.; Heemstra, J. M. *WIREs Nanomed Nanobiotechnol* **2015**, *7*, 282−297. (b) Korri-Youssoufi, H.; Garnier, F.; Srivastava, P.; Godillot, P.; Yassar, A. *J. Am. Chem. Soc.* **1997**, *119*, 7388−7389. (c) Lu, X.; Watts, E.; Jia, F.; Tan, X.; Zhang, K. *J. Am. Chem. Soc.* **2014**, *136*, 10214−10217. (d) Tan, X.; Li, B. B.; Lu, X.; Jia, F.; Santori, C.; Menon, P.; Li, H.; Zhang, B.; Zhao, J. J.; Zhang, K. *J. Am. Chem. Soc.* **2015**, *137*, 6112−6115.
(24) (a) Kwak, M.; Herrmann, A. *Angew. Chem., Int. Ed.* **2010**, *49*, 8574−8587. (b) Peng, L.; Wu, S.; You, M.; Han, D.; Chen, Y.; Fu, T.; Tan, W. *Chem. Sci.* **2013**, *4*, 1928−1938.
(25) (a) Watson, K. J.; Park, S.-J.; Im, J.; Nguyen, S. T.; Mirkin, C. A. *J. Am. Chem. Soc.* **2001**, *123*, 5592−5593. (b) Gibbs, J. M.; Park, S.-J.; Anderson, D. R.; Watson, K. J.; Mirkin, C. A.; Nguyen, S. T. *J. Am. Chem. Soc.* **2005**, *127*, 1170−1178. (c) Gibbs-Davis, J. M.; Schatz, G. C.; Nguyen, S. T. *J. Am. Chem. Soc.* **2007**, *129*, 15535−15540. (d) Park, S. Y.; Gibbs-Davis, J. M.; Nguyen, S. T.; Schatz, G. C. *J. Phys. Chem. B* **2007**, *111*, 8785−8791. (e) Lytton-Jean, A. K. R.; Gibbs-Davis, J. M.; Long, H.; Schatz, G. C.; Mirkin, C. A.; Nguyen, S. T. *Adv. Mater.* **2009**, *21*, 706−709.
(26) Vyborna, Y.; Vybornyi, M.; Rudnev, A. V.; Häner, R. *Angew. Chem., Int. Ed.* **2015**, *54*, 7934−7938.
(27) Häner, R.; Garo, F.; Wenger, D.; Malinovskii, V. L. *J. Am. Chem. Soc.* **2010**, *132*, 7466−7471.
(28) Aida, T.; Meijer, E.; Stupp, S. I. *Science* **2012**, *335*, 813−817.
(29) Busseron, E.; Ruff, Y.; Moulin, E.; Giuseppone, N. *Nanoscale* **2013**, *5*, 7098−7140.
(30) Yang, L.; Tan, X.; Wang, Z.; Zhang, X. *Chem. Rev.* **2015**, *115*, 7196−7239.
(31) van der Zwaag, D.; de Greef, T. F. A.; Meijer, E. W. *Angew. Chem., Int. Ed.* **2015**, *54*, 8334−8336.
(32) Görl, D.; Zhang, X.; Stepanenko, V.; Würthner, F. *Nat. Commun.* **2015**, *6*, 7009.
(33) Mukhopadhyay, R. D.; Ajayaghosh, A. *Science* **2015**, *349*, 241−242.
(34) Huang, F.; Scherman, O. A. *Chem. Soc. Rev.* **2012**, *41*, 5879−5880.
(35) Vybornyi, M.; Rudnev, A. V.; Langenegger, S. M.; Wandlowski, T.; Calzaferri, G.; Häner, R. *Angew. Chem., Int. Ed.* **2013**, *52*, 11488−11493.
(36) Vybornyi, M.; Rudnev, A.; Häner, R. *Chem. Mater.* **2015**, *27*, 1426−1431.
(37) (a) Micali, N.; Vybornyi, M.; Mineo, P.; Khorev, O.; Häner, R.; Villari, V. *Chem. - Eur. J.* **2015**, *21*, 9505−9513. (b) Pescitelli, G.; Di Bari, L.; Berova, N. *Chem. Soc. Rev.* **2014**, *43*, 5211−5233.
(38) Endo, M.; Sugita, T.; Katsuda, Y.; Hidaka, K.; Sugiyama, H. *Chem. - Eur. J.* **2010**, *16*, 5362−5368.
(39) Wang, R.; Kuzuya, A.; Liu, W.; Seeman, N. C. *Chem. Commun.* **2010**, *46*, 4905−4907.
(40) Nakata, M.; Zanchetta, G.; Chapman, B. D.; Jones, C. D.; Cross, J. O.; Pindak, R.; Bellini, T.; Clark, N. A. *Science* **2007**, *318*, 1276−1279.
(41) Lilley, D. M. J. *Q. Rev. Biophys.* **2000**, *33*, 109−159.
(42) *Oxford Handbook of Nucleic Acid Structure*; Neidle, S.; Oxford University Press: New York, 1999.
(43) Bloomfield, V. A.; Crothers, D. M.; Tinoco, I. *Nucleic Acids - Structures, Properties, and Functions*; University Science Books: Sausalito, 2000.
(44) SantaLucia, J.; Hicks, D. *Annu. Rev. Biophys. Biomol. Struct.* **2004**, *33*, 415−440.
(45) Saenger, W. *Principles of Nucleic Acid Structure*; Springer-Verlag: New York, 1984.
(46) Protozanova, E.; Yakovchuk, P.; Frank-Kamenetskii, M. D. *J. Mol. Biol.* **2004**, *342*, 775−785.

DOI: 10.1021/jacs.5b09889
J. Am. Chem. Soc. 2015, 137, 14051−14054